

Quantum dynamics of a two-level emitter with a modulated transition frequency

Mihai Macovei^{1,2,*} and Christoph H. Keitel^{1,†}¹*Max-Planck-Institut für Kernphysik, Saupfercheckweg 1, D-69117, Heidelberg, Germany*²*Institute of Applied Physics, Academy of Sciences of Moldova, Academiei strasse 5, MD-2028, Chişinău, Moldova*

(Received 8 August 2014; published 20 October 2014)

The resonant quantum dynamics of an excited two-level emitter is investigated via classical modulation of its transition frequency while simultaneously the radiator interacts with a broadband electromagnetic field reservoir. The frequency of modulation is selected to be of the order of the bare-state spontaneous decay rate. In this way, one can induce quantum interference effects, and consequently, quantum coherences among multiple decaying transition pathways. Depending on the modulation depth and its absolute phase, both the spontaneous emission and the frequency shift may be conveniently modified and controlled.

DOI: [10.1103/PhysRevA.90.043838](https://doi.org/10.1103/PhysRevA.90.043838)

PACS number(s): 42.50.Lc, 37.30.+i, 42.50.Pq, 42.25.Hz

I. INTRODUCTION

Spontaneous emission is a well established fundamental phenomenon [1–4]. It occurs due to the interaction of excited emitters with the vacuum modes of the environmental electromagnetic field reservoir. Useful applications of spontaneous radiation control may arise, for instance, in higher-frequency coherent light generation [5,6] or spontaneous parametric down-conversion processes [7]. On the other side, spontaneous emission often plays a negative role in quantum processing of information [8]. Therefore, it is not surprising that a significant amount of work is carried out regarding its control. Particularly, earlier approaches to influence the spontaneous emission were by using optical cavities [9–11]. A modern and more advanced version of those ideas consists in using photonic crystals environments where photon forbidden bands occur leading to spontaneous emission inhibition or localization [12–14]. Infrequent application to a two-level atom of microwave pulses [15] or sequence of pulses [16], or rather intense low-frequency coherent fields [17] (see also Ref. [18]) lead to spontaneous emission control as well. Quenching of spontaneous emission occurs as well via involving quantum interference effects between various decaying pathways which are dependent on mutual orientation of corresponding transition dipoles [4,19,20]. Furthermore, the Lamb shift of laser-dressed atomic states and quantum interferences due to energy shifts and their effect on spontaneous emission were investigated also in Refs. [21,22]. One can also control the spontaneous emission by periodically shifting the atomic transition frequency from the atom-cavity resonance [23,24] or via coupling a single state to a continuum of many states [25,26]. Remarkably, periodically perturbed atomic transitions lead to a number of fascinating effects such as induced transparency or extreme ultrashort pulses, respectively [27].

Here, we demonstrate the suppression of spontaneous decay of a two-level system (qubit) that is embedded in a broadband electromagnetic field reservoir and is subjected to an intense, time-dependent, frequency modulation driving force. The suppression is a direct consequence of quantum interference

effects induced by the modulation. A frequency shift to the transition frequency is induced as well. Furthermore, the absolute phase of the modulation can be a convenient tool to control these processes. Coherent modulation of the transition frequency leads to appearance of new decay channels that may interfere destructively contributing to spontaneous emission inhibition (see Fig. 1). This occurs when the frequency of modulation is of the order of the bare-state qubit's decay rate or less. The spontaneous emission is described by an exponential decaying law with a time-dependent decay rate and exhibiting plateaus with a very slow decoherence rate. The quantum decoherence due to spontaneous emission can be further minimized via stronger frequency modulation depths. Moreover, the induced time-dependent frequency shift depends on external control parameters, such as the applied intensity and the external field amplitude absolute phase, and can be influenced accordingly. It vanishes, however, at resonance and in the absence of quantum interference effects due to frequency modulation processes. In a free-space setup, the spontaneous emission inhibition is less probable via transition frequency modulation of an excited two-level emitter. This deviation from Ref. [17] arises because our treatment is classical and especially limited to moderately intense modulating fields.

Our system can be implemented, for example, via off-resonant laser driving of a two-level emitter [17,23–28]. One can apply a laser field with a high nonresonant frequency ω' and possessing a periodically modulated amplitude of the field strength $\epsilon(t) = \epsilon_0 \cos(\omega t + \phi) \cos(\omega' t)$ with $\omega \ll \omega_0 \ll \omega'$ to a two-level atom of frequency ω_0 . Then a modulated shift $\Delta\omega_0$ of the transition frequency is achieved via the quadratic Stark effect, i.e., $\Delta\omega_0 = b \cos^2(\omega t + \phi)$, where b is the modulation amplitude. Additional systems can be molecules or quantum dots, even those possessing permanent dipoles [29–34]. When pumped with an intense low-frequency coherent field, the amplitude of the frequency modulation will be proportional to the magnitude of the permanent dipole multiplied by the external field strength. An alternative scheme can be as well a two-level quantum dot embedded in a broadband microcavity and interacting with a surface acoustic wave coherently modulating its transition frequency [35]. Superconducting qubits with periodically perturbed transition frequencies and weakly coupled with a quantum LC circuit or a nanomechanical resonator are suitable candidates as well [36].

*macovei@phys.asm.md

†keitel@mpi-hd.mpg.de

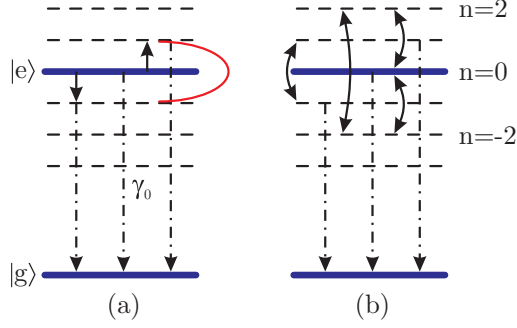


FIG. 1. (Color online) Schematic diagram of a two-level emitter with modulated transition frequency (a) without and (b) with showing the involved quantum coherences among specific transition pathways. Due to modulation, multiple induced decaying channels $n = 0, \pm 1, \pm 2, \dots$, interfere such that spontaneous emission is slowed down. γ_0 is the single-qubit spontaneous decay rate in the absence of modulation.

The article is organized as follows. In Sec. II we describe the analytical approach and the system of interest, while in Sec. III we analyze the obtained results. The summary given in Sec. IV is followed by two Appendixes.

II. APPROACH

The Hamiltonian $H = H_0 + H_I$ describing the system of interest can be represented via (see Refs. [23,24] for a detailed derivation for the analogous case with usual vacuum Appendix A)

$$H_0 = \sum_k \hbar \omega_k a_k^\dagger a_k + \hbar [\omega_0 + b \cos(\omega t + \phi)] S_z,$$

$$H_I = i \sum_k (\vec{g}_k \cdot \vec{d})(a_k^\dagger S^- - a_k S^+), \quad (1)$$

where the first term H_0 , characterizes the free Hamiltonian of the electromagnetic field (EMF) as well as of the qubit subsystem with modulated transition frequency whereas the second one, i.e., H_I , accounts for the interaction of the two-level qubit with the vacuum modes of the environmental electromagnetic field reservoir. Here, $S^+ = |e\rangle\langle g|$, $S^- = [S^+]^\dagger$ and $S_z = (|e\rangle\langle e| - |g\rangle\langle g|)/2$ are the well-known quasispin operators obeying the commutation relations $[S^+, S^-] = 2S_z$ and $[S_z, S^\pm] = \pm S^\pm$. The creation a_k^\dagger and annihilation a_k electromagnetic field operators satisfy the commutation relations $[a_k, a_{k'}^\dagger] = \delta_{kk'}$ and $[a_k, a_{k'}] = [a_k^\dagger, a_{k'}^\dagger] = 0$. Further, ω_0 is the qubit's transition frequency $|e\rangle \leftrightarrow |g\rangle$ (see Fig. 1) in the absence of classical modulation, while b is the modulation amplitude with frequency ω and phase ϕ . The two-level emitter possessing the transition dipole moment d couples with the vacuum modes via the coupling constant g_k . In the following, we perform a unitary transformation

$$U = \exp \left\{ \frac{i}{\hbar} \int_0^t d\tau \tilde{H}_0(\tau) \right\}, \quad (2)$$

with $\tilde{H}_0(\tau) = \sum_k \hbar \omega_0 a_k^\dagger a_k + \hbar [\omega_0 + b \cos(\omega \tau + \phi)] S_z$ and arrive at the Hamiltonian

$$\tilde{H} = \sum_k \hbar (\omega_k - \omega_0) a_k^\dagger a_k + i \sum_k \sum_{m=-\infty}^{\infty} (\vec{g}_k \cdot \vec{d}) J_m(\chi) \times (a_k^\dagger S^- e^{-im(\omega t + \phi)} - a_k S^+ e^{im(\omega t + \phi)}), \quad (3)$$

where $\chi = b/\omega$ while $J_m(\chi)$ is the corresponding ordinary Bessel function. Here, we used the expansion via the m th-order Bessel function of the first kind, i.e., $\exp\{\pm i \chi \sin(\omega t + \phi)\} = \sum_{m=-\infty}^{\infty} J_m(\chi) \exp[\pm im(\omega t + \phi)]$ as well as the notation $S^\pm e^{\mp i \chi \sin \phi} \equiv \tilde{S}^\pm$, and dropped the tilde afterwards.

In the weak qubit-environment coupling limit, one can obtain the master equation describing the quantum dynamics of any atomic operator Q . For this, we use the standard elimination procedure of the electromagnetic field operators from the Heisenberg equation

$$\frac{d}{dt} \langle Q \rangle = \frac{i}{\hbar} \langle [\tilde{H}, Q] \rangle, \quad (4)$$

where the notation $\langle \dots \rangle$ indicates averaging over the initial state of both the qubit and the surrounding electromagnetic field bath [1–4]. As an environmental electromagnetic field reservoir, we consider a broadband optical cavity possessing the frequency ω_c , qubit-cavity coupling being g , and a cavity leaking constant denoted by κ (the free-space situation is described in Appendix A). Thus, the Heisenberg equations for the field operators are

$$\frac{d}{dt} a^\dagger(t) = (i\delta_c - \kappa) a^\dagger + \sum_{n=-\infty}^{\infty} g J_n(\chi) S^+(t) e^{in(\omega t + \phi)}, \quad (5)$$

with $a(t) = [a^\dagger(t)]^\dagger$ and $\delta_c = \omega_c - \omega_0$. Its formal solution in the weak-coupling limit is $a^\dagger(t) = a_v^\dagger(t) + a_s^\dagger(t)$, where $a_v^\dagger(t) = a^\dagger(0) e^{-(\kappa - i\delta_c)t}$ while

$$a_s^\dagger(t) = \sum_{n=-\infty}^{\infty} g J_n(\chi) \int_0^t dt' e^{-(\kappa - i\delta_c)(t-t')} \times S^+(t') e^{in(\omega t' + \phi)}. \quad (6)$$

In the Markov approximation we have $S^+(t') \approx S^+(t)$. Then the integral

$$\int_0^t dt' e^{(\kappa - i\delta_c)t'} e^{in\omega t'} = \frac{e^{(\kappa - i(\delta_c - n\omega))t} - 1}{\kappa + i(n\omega - \delta_c)}.$$

Inserting this expression in Eq. (6) and keeping only the slower contributions, that is, we are interested in frequency modulation regimes slower than the cavity decay rate, i.e., $\omega \ll \kappa$, one arrives at

$$a^\dagger(t) = a^\dagger(0) e^{-(\kappa - i\delta_c)t} + \sum_{n=-\infty}^{\infty} \frac{g J_n(\chi)}{\kappa + i(n\omega - \delta_c)} \times S^+(t) e^{in(\omega t + \phi)}. \quad (7)$$

Then, one can write down the master equation for an arbitrary mean value of a qubit operator Q that can be obtained after introducing Eq. (3) in the corresponding Heisenberg equation,

i.e., Eq. (4)

$$\begin{aligned} \langle \dot{Q} \rangle = & - \sum_{m=-\infty}^{\infty} g J_m(\chi) \{ \langle a^\dagger [S^-, Q] \rangle e^{-im(\omega t + \phi)} \\ & + \langle [Q, S^+] a \rangle e^{im(\omega t + \phi)} \}, \end{aligned} \quad (8)$$

where an overdot denotes differentiation with respect to time. Introducing Eq. (7) in the master equation (8) and taking into account that $\langle a^\dagger(0) \dots \rangle = 0$ and $\langle \dots a(0) \rangle = 0$ one obtains

$$\begin{aligned} \langle \dot{Q} \rangle = & i\Omega(t) \langle [S_z, Q] \rangle - \gamma(t) \{ \langle S^+ [S^-, Q] \rangle \\ & + \langle [Q, S^+] S^- \rangle \}. \end{aligned} \quad (9)$$

The operator form of Eq. (9) looks standard, i.e., of Lindblad form [3,37], with, however, time-dependent coefficients, namely,

$$\begin{aligned} \Omega(t) = & \sum_{\{m,n\}=-\infty}^{\infty} \bar{\delta}_n J_m(\chi) J_n(\chi) \cos[(n-m)(\omega t + \phi)], \\ \gamma(t) = & \sum_{\{m,n\}=-\infty}^{\infty} \bar{\gamma}_n J_m(\chi) J_n(\chi) \cos[(n-m)(\omega t + \phi)], \end{aligned} \quad (10)$$

with

$$\bar{\delta}_n = \frac{(n\omega - \delta_c)g^2}{\kappa^2 + (n\omega - \delta_c)^2}, \quad \text{and} \quad \bar{\gamma}_n = \frac{\gamma_0 \kappa^2}{\kappa^2 + (n\omega - \delta_c)^2}. \quad (11)$$

Here, $\Omega(t)$ and $\gamma(t)$ describe the time-dependent frequency shift and spontaneous decay process, respectively, while $\gamma_0 = g^2/\kappa$ is the near-resonance single-qubit spontaneous decay rate without frequency modulation, i.e., when $\chi = 0$. In the numerical simulations we truncate the summation range $(-\infty, \infty)$ to $(-\bar{n}, \bar{n})$. This is justified as $\bar{\gamma}_n \sim 1/[\kappa^2 + (n\omega)^2]$ for near qubit-cavity resonance. Concretely, \bar{n} is chosen such that the results converge, i.e., remain unchanged if one further increases \bar{n} . Note that this is not the case for vacuum free-space setups (see Appendix A). Furthermore, to avoid unphysical results [38], \bar{n} should be the same for both indices and, also, Eq. (9) should be independent of the exchange of indices, i.e., $m \leftrightarrow n$.

The population quantum dynamics of an initially excited two-state radiator can be easily obtained from Eq. (9), namely,

$$\langle S_z(t) \rangle = \exp[-2\Gamma(t)] - 1/2, \quad (12)$$

with a generalized spontaneous decay rate given by

$$\Gamma(t) = \int_0^t \gamma(\tau) d\tau.$$

One can see here that the qubit inversion obeys a modified exponential decay law with a time-dependent decay rate. In the absence of frequency modulation, i.e., $\chi = 0$, one recovers the standard exponential law near qubit-cavity resonance [4]

$$\langle S_z(t) \rangle = \exp[-2\gamma_0 t] - 1/2. \quad (13)$$

Thus, the periodical modulation of the qubit's transition frequency modifies the spontaneous decay.

In the following section, we shall describe the quantum dynamics of an excited two-level emitter with modulated transition frequency.

III. RESULTS AND DISCUSSION

We proceed to investigate the qubit's dynamics based on Eqs. (7) to (12). One can observe from Eq. (7) that the atomic dipole may oscillate at frequencies $\omega_n = \omega_0 + n\omega$, where n is an arbitrary integer number including zero. This means that photons at these frequencies are generated that can lead to interference effects. Indeed, inspecting Eq. (9), one can realize that the two-level emitter with the frequency modulation is reduced to an equivalent system containing multiple excited dressed levels, $\omega_0 \pm |n\omega|$ $\{n = 0, 1, 2, \dots\}$, decaying to the ground state (see Fig. 1). When the dressed-state splitting is of the order of the cavity mediated radiator's decay rate γ_0 then quantum interferences occur among various transition decay paths. For instance, in Fig. 1(a) the two decay channels $\omega_0 \pm \omega$ interfere leading to appearance of quantum coherences schematically shown in Fig. 1(b). Technically, due to the Bessel function property, $J_{-n}(x) = (-1)^n J_n(x)$, some of the terms from expressions (10) cancel each other while others add up. To illustrate this we chose the simplest case $\bar{n} = 1$ and $\delta_c = 0$, and then the expression for $\gamma(t)$ takes the form

$$\begin{aligned} \gamma(t)/\gamma_0 = & J_0^2(\chi) + \kappa^2 \{ J_1(\chi) J_1(\chi) + J_{-1}(\chi) J_{-1}(\chi) \\ & + 2J_{-1}(\chi) J_1(\chi) \cos[2(\omega t + \phi)] \} / (\kappa^2 + \omega^2). \end{aligned} \quad (14)$$

The first three terms from Eq. (14) describe the spontaneous emission processes on the induced transitions $|e, n = 0\rangle \rightarrow |g\rangle$ and $|e, n = \pm 1\rangle \rightarrow |g\rangle$, respectively [see Fig. 1(a)]. The last term in Eq. (14) takes into account the cross correlations among the spontaneously decaying channels [see Fig. 1(b), where n denotes a particular sublevel] $|e, n = 1\rangle \rightarrow |g\rangle$ and $|e, n = -1\rangle \rightarrow |g\rangle$ or vice versa (and, hence, a prefactor of 2 there), i.e., characterizes quantum decay interference effects [4]. On the other hand, the cross-decaying correlations among the transition paths $|e, n = 0\rangle \rightarrow |g\rangle$ and $|e, n = \pm 1\rangle \rightarrow |g\rangle$ reciprocally cancel each other. Obviously, this illustration scheme can be extended to $\bar{n} > 1$ [see Fig. 1(b) showing the induced coherences for $\bar{n} = 2$]. These processes together with frequency modulation dressing of the multiple decaying rates will lead to a slowing down of the spontaneous emission processes that are also absolute phase dependent. Notice that for $\chi \gg 1$ the n th-order Bessel function of the first kind can be represented as [39]

$$J_n(\chi) \approx \sqrt{\frac{2}{\pi\chi}} \cos(\chi - \pi n/2 - \pi/4), \quad \text{when } n < \chi. \quad (15)$$

The dependence $J_n(\chi) \propto 1/\sqrt{\chi}$ will also explain the quenching of the spontaneous decay processes for larger modulation depths. This tendency persists even in the absence of quantum coherences due to cross-damping effects. If $n > \chi \gg 1$ the spontaneous decay rate tends to even lower values due to the prefactor $1/[\kappa^2 + (n\omega)^2]$.

Figure 2 shows the population kinetics of an excited two-level emitter given by Eq. (12) for some parameters of interest. Particularly, the short-dashed line depicts the typical exponential spontaneous decay law in the absence of frequency modulation which is characterized by Eq. (13). The solid and long-dashed curves describe the spontaneous decay processes

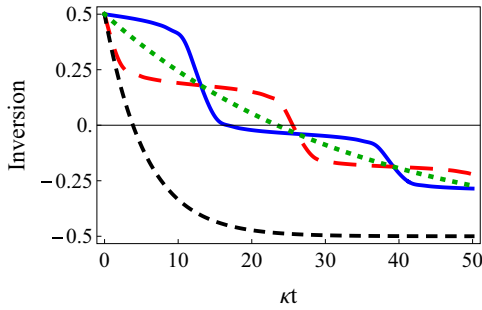


FIG. 2. (Color online) The time dependence of the mean value of the inversion operator $\langle S_z(t) \rangle$ as a function of κt . Here the solid line corresponds to $\chi = 50$ and $\phi = 0$, the long-dashed one to $\chi = 50$ and $\phi = \pi/2$ while the dotted curve to $\chi = 50$ without taking into account quantum coherences. The short-dashed line depicts the usual spontaneous decay, i.e., when $\chi = 0$. Other parameters are $g = 0.3\kappa$, $\omega = 0.12\kappa$, $\delta_c = 0$, and $\kappa = 1$.

when the transition frequency is modulated with a modulation depth $\chi = 50$ and a phase $\phi = 0$ or $\phi = \pi/2$, respectively. The phase dependence is a clear evidence of quantum interference effects. This occurs for stronger modulation depths χ and when the frequency of modulation ω is comparable to or less than the single-qubit decay rate γ_0 , and $\{\omega, \gamma_0\} \ll \kappa$. For the sake of comparison, the dotted curve characterizes the spontaneous emission behavior without taking into account the quantum coherences due to cross-damping effects [see Fig. 1(a)], that is, in Eq. (13) we have taken

$$\tilde{\gamma} = \sum_{n=-\bar{n}}^{\bar{n}} \tilde{\gamma}_n J_n^2(\chi), \quad [\text{see Eq. (10)}],$$

instead of γ_0 . Thus, concluding, the cross-damping effects [i.e., the terms with $n \neq m$ in Eqs. (10) and (12); see, also, Fig. 1(b)] contribute considerably to the final spontaneous decay processes (compare the solid, dotted, and the long-dashed curves in Fig. 2, respectively).

The population behaviors shown in Fig. 2 are in accordance with the time dependence form of $\gamma(t)$ given in Eq. (10). The almost decoherence-free plateaus observed in Fig. 2 correspond to lower values of $\gamma(t)$ (see Fig. 3). The inhibition of

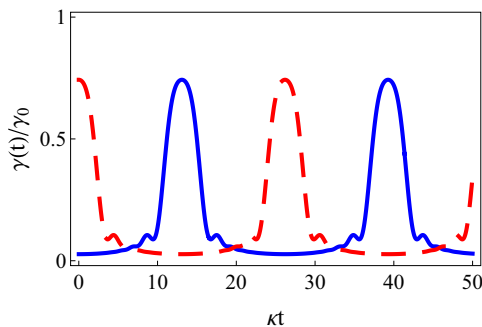


FIG. 3. (Color online) The time dependence of the decay rate $\gamma(t)$ given in Eq. (10) versus κt . Here the solid line corresponds to $\chi = 50$ and $\phi = 0$ whereas the long-dashed line one to $\chi = 50$ and $\phi = \pi/2$. Other parameters are the same as in Fig. 2.

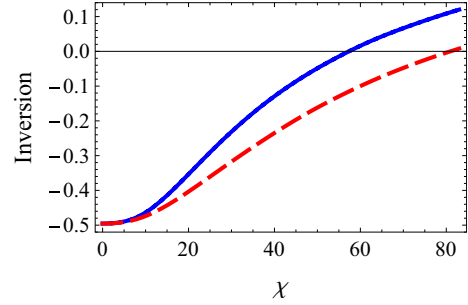


FIG. 4. (Color online) The mean value of the inversion operator $\langle S_z(t) \rangle$ versus the modulation depth χ when $\kappa t = 30$. Here the solid line corresponds to $\phi = 0$, while the long-dashed line one to $\phi = \pi/2$. Other parameters are the same as in Fig. 2.

the spontaneous decay can be further improved by increasing the modulation depth χ . Therefore, in Fig. 4, we have fixed the evolution time at $\kappa t = 30$ and changed the modulation depth χ accordingly. At lower modulation amplitudes, or in its absence, the qubit is in the ground state at this evolution stage. As it was already mentioned, stronger modulation depths contribute to a further slowing of the quantum decoherence. The reason is the interplay between interference effects among multiple decay channels described above and the frequency modulation dressing of the corresponding decay rates [see Eq. (15)]. Note, however, that the opposite case, i.e., $\omega \gg \kappa$, does not show any time or phase dependence in the parameters entering in Eq. (9) or Eq. (12) and, consequently, no quantum interference effects among the different transition pathways occur. This situation was nicely investigated in Refs. [23,24], respectively.

We shall further focus on discussions around the frequency shift due to periodical modulation of the transition frequency. Therefore, the frequency shift $\Omega(t)$, given in Eq. (10), is plotted in Fig. 5 for particular parameters. Here, again, one can observe phase-dependent behaviors due to induced quantum coherences. Particularly, when $\bar{n} = 1$ and $\delta_c = 0$, we have from Eqs. (10) and (11)

$$\Omega(t) = \bar{\Omega} J_0(\chi) \{J_1(\chi) - J_{-1}(\chi)\} \cos(\omega t + \phi), \quad (16)$$

where $\bar{\Omega} = g^2 \omega / (\kappa^2 + \omega^2)$. One can observe here that the frequency shift is due to cross correlations among the transition channels $|e, n = 0\rangle \rightarrow |g\rangle$ and $|e, n = \pm 1\rangle \rightarrow |g\rangle$,

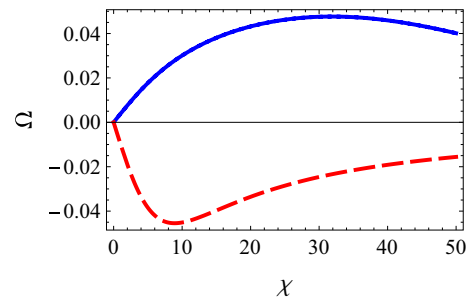


FIG. 5. (Color online) The frequency shift Ω (in units of κ) as a function of modulation depth χ when $\kappa t = 10$. Here the solid line corresponds to $\phi = 0$, while the long-dashed line to $\phi = \pi/2$. Other parameters are the same as in Fig. 2.

respectively, i.e., opposite to spontaneous emission contributions where these processes cancel out. Evidently, these discussions can be generalized for $\bar{n} > 1$. Notice that this frequency shift vanishes in the absence of transition frequency modulation at resonance, i.e., $\chi = 0$, or when $\omega \gg \kappa$ at $\delta_c = 0$.

For an experimental realization of the proposed scheme we need moderate modulation depths. This can be achieved, for instance, in molecular or quantum dot systems possessing a permanent dipole d_p as it was also mentioned in the article. For $d_p \gg d$ and E_L being the amplitude strength of the applied low-frequency coherent field, one can obtain the necessary modulation depth $b \propto (d_p E_L)$ that is smaller than the transition frequency of the two-level qubit while $\chi \gg 1$. In asymmetrical quantum dot systems the permanent dipole is proportional to the size of the quantum dot and this can be used in engineering of the required model [30–33]. Certain molecules possess this property also, i.e., $d_p \gg d$ [29,34].

Finally, while we have considered a broad-band cavity environmental reservoir, the multiple induced decay interference approach developed may also be applied for quantized vacuum modes of free-space in a related setup [17], for instance. There, applying a quantized and sufficiently strong low-frequency field beyond applicability here, to a two-level atom including far-off resonant states in free space, one can induce quantum interferences among few-photon induced transitions. Those process's scaling show an interplay between different relevant detunings and applied intensity strengths such that one can stop at a particular \bar{n} -photon process [17] (see Appendix B).

IV. SUMMARY

Summarizing, we have demonstrated how quantum decay interference phenomena induced among multiple decaying channels occurring due to moderately intense transition frequency modulation of a two-level emitter embedded in a broadband electromagnetic field reservoir together with frequency modulation dressing of the spontaneous decay rates can suppress quantum dissipations due to spontaneous emission. Particularly, phase-dependent low decoherence plateaus appear in such a process. Furthermore, a generalized cross-correlated frequency shift to the two-level qubit's transition frequency is induced here as well.

ACKNOWLEDGMENTS

We acknowledge the financial support by the German Federal Ministry of Education and Research, Grant No. 01DK13015, and Academy of Sciences of Moldova, Grant No. 13.820.05.07/GF. Furthermore, we benefited from useful discussions with Jörg Evers, particularly on the employed weak-field limit as compared to that of Ref. [17]. M.M. is grateful to the Theory Division of the Max Planck Institute for Nuclear Physics from Heidelberg, Germany, for kind hospitality.

APPENDIX A: MASTER EQUATION WITH A MODULATED TRANSITION IN FREE SPACE

In this Appendix, we shall focus on the spontaneous decay of an excited two-level emitter with modulated transition

frequency via usual vacuum modes of the EMF reservoir. The purpose is to show that an unshaped vacuum is not sufficient for the spontaneous emission suppression investigated here. For convenience we derive the modulation Hamiltonian entering in Eq. (1). For this, one considers that a moderately strong low-frequency coherent field is applied to a two-state atom being initially in its excited state. The Hamiltonian of this process is

$$H = \sum_k \hbar \omega_k a_k^\dagger a_k + \hbar \omega_0 S_z + \hbar \Omega \cos(\omega t)(S^+ + S^-) + i \sum_k (\vec{g}_k \cdot \vec{d})(a_k^\dagger - a_k)(S^+ + S^-). \quad (\text{A1})$$

Here, ω_0 is the transition frequency among the states $|e\rangle \leftrightarrow |g\rangle$ while Ω is the corresponding Rabi frequency with ω being the frequency of the external applied low-frequency coherent field. The atom-vacuum coupling strength is $\vec{g}_k = \sqrt{2\pi \hbar \omega_k / V} \vec{e}_\lambda$, where V is quantized volume while \vec{e}_λ is the photon polarization vector with $\{\lambda = 1, 2\}$.

We apply a unitary transformation to the Hamiltonian (A1), i.e., $H \equiv U(t) H U^{-1}(t)$, where $U(t) = \exp[i \frac{\Omega}{\omega} \sin(\omega t)(S^+ + S^-)]$. This transformation is useful as it allows to represent the Hamiltonian via the n -photon processes involved, namely,

$$H = \hbar \omega_0 S_z \sum_{n=0}^{\infty} J_n(\rho) \cos(n\omega t)[1 + (-1)^n(1 - \delta_{n,0})] + \frac{i}{2} \hbar \omega_0 (S^- - S^+) \sum_{n=1}^{\infty} J_n(\rho) \sin(n\omega t)[1 - (-1)^n] + \sum_k \hbar \omega_k a_k^\dagger a_k + i \sum_k (\vec{g}_k \cdot \vec{d})(a_k^\dagger - a_k)(S^+ + S^-), \quad (\text{A2})$$

where $\rho = 2\Omega/\omega$. It is easy to observe that the even-photon processes with $n = 2, 4, \dots$, correspond to modulation of the transition frequency, while the odd-photon processes, i.e., $n = 1, 3, \dots$, lead to induced transitions among the involved energy levels. For our purposes one requires $\rho \ll 1$ as well as $\omega \ll \omega_0$. Under these restrictions, i.e., taking into account that

$$J_n(\rho) \approx \rho^n \left\{ \frac{2^{-n}}{\Gamma(1+n)} - \frac{2^{-2-n} \rho^2}{(1+n)\Gamma(1+n)} + O[\rho^4] \right\},$$

the working Hamiltonian is

$$H = \sum_k \hbar \omega_k a_k^\dagger a_k + \hbar[\omega_0 + b \cos(2\omega t) + b' \cos(4\omega t)] S_z + i \sum_k (\vec{g}_k \cdot \vec{d})(a_k^\dagger - a_k)(S^+ + S^-). \quad (\text{A3})$$

Here, $b = \omega_0 \rho^2/4$, $b' = \omega_0 \rho^4/192$, and $\omega_0 \equiv \omega_0(1 - \rho^2/4)$. Thus, we have considered that the frequency modulation takes place via two- and four-photon processes, simultaneously, while higher-photon effects are negligible because one can always select a system with $\omega_0 \rho^n/\omega \ll \omega_0 \rho^{n-2}/\omega$, and for an even n with $n > 4$. Furthermore, the induced transitions through odd-photon processes among the involved energy levels do not occur because of the off-resonance, and therefore, are ignored here [i.e., the second line of the Hamiltonian (A2)].

The master equation describing the spontaneous decay of a two-level radiator with modulated transition frequency in free-space according to the Hamiltonian (A3) and in the Born-Markov, dipole, and rotating-wave approximations has the form

$$\frac{d}{dt}\langle Q(t) \rangle = -(\gamma_f(t) - i\Omega_f(t))\langle S^+[S^-, Q] \rangle + \text{H.c.}, \quad (\text{A4})$$

where

$$\begin{aligned} & \gamma_f(t) - i\Omega_f(t) \\ &= \sum_{n, n'=-n_0}^{n_0} \sum_{m, m'=-m_0}^{m_0} J_n(\chi) J_{n'}(\chi) J_m(\chi') J_{m'}(\chi') \\ & \quad \times (\gamma_{0n'm'} - i\Omega_{0n'm'}) e^{-2i\omega t(n-n')} e^{-4i\omega t(m-m')}, \end{aligned}$$

with

$$\begin{aligned} \Omega_{0n'm'} &= \sum_k \frac{(\vec{g}_k \cdot \vec{d})^2}{\hbar^2} P \frac{1}{\omega_k - \omega_0 - 2n'\omega - 4m'\omega}, \\ \gamma_{0n'm'} &= \gamma \left(1 + \frac{2n'\omega}{\omega_0} + \frac{4m'\omega}{\omega_0} \right)^3, \end{aligned}$$

and $\chi = b/(2\omega)$, while $\chi' = b'/(4\omega)$.

Here, P is the Cauchy principal value, while $2\gamma = 4d^2\omega_0^3/(3\hbar c^3)$ is the free-space single-atom spontaneous decay rate in the absence of frequency modulation [4].

In the following, we consider that $\chi \gg 1$ while $\chi' \ll 1$, i.e., the frequency modulation via simultaneous four-photon processes are negligible. This can be achieved in the weak field regime, for example, when $\rho = 2 \times 10^{-1}$ and $\omega_0/\omega = 2 \times 10^4$, that is, one has $\chi = 10^2$ while $\chi' \approx 4.2 \times 10^{-2}$. For this reason we do not expect to obtain the quantum interference effects without a cavity like in Ref. [17]. Thus, the motivation to keep the modulation of the transition frequency due to a simultaneous four-photon process in the Hamiltonian (A3) as well as in the master equation (A4), i.e., the term proportional to b' , was to show that spontaneous decay via the induced absorption or emission of four photons is taking place also due to transition frequency modulation via a two-photon process described by b (for instance, when $n_0 = 2$). This latter process is more probable than the corresponding one due to b' .

Figure 6 shows the spontaneous decay law of an excited atom in free space, i.e., $\langle S_z(t) \rangle = \exp[-2\Gamma_f(t)] - 1/2$ where

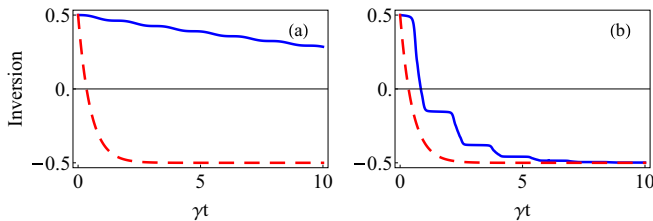


FIG. 6. (Color online) The free-space mean-value of the inversion operator $\langle S_z(t) \rangle$ versus γt . Here, $\rho = 0.2$, $\omega/\gamma = 1$, $\phi = 0$ while $\omega_0/\omega = 2 \times 10^4$ and, hence, $\chi = 100$. (a) $n_0 = 1$; (b) $n_0 = 50$. The dashed line shows the usual free-space spontaneous decay law in the absence of frequency modulation.

$\Gamma_f(t) = \int_0^t \gamma_f(\tau) d\tau$ with $m = m' = 0$, when $n_0 = 1$ and $n_0 = 50$, respectively, and for some particular parameters of interest. While the spontaneous decay is clearly slowed down for $n_0 \ll \chi > 1$ one cannot predict what is the particular value of n_0 which would be realized in a real experiment. Furthermore, larger values of n_0 with a fixed $\chi = 100$ do not lead to spontaneous emission inhibition. Thus, it is unlikely that the spontaneous emission will be inhibited in free space via transition frequency modulation of an excited two-level emitter unless and until we are not able to select a particular n_0 -photon process.

APPENDIX B: SPONTANEOUS DECAY MODIFICATION VIA APPLYING A STRONG QUANTIZED LOW-FREQUENCY FIELD

In Ref. [17] a related mechanism was discussed where an effective two-level system was driven with a quantum field with frequency ω of the order of the linewidth of the considered transition. Since in reality the low-frequency field will also couple off-resonantly to all transitions in the atom, one can justify a Hamilton operator with extra interference terms as indicated in detail in the Ref. [17] with the consequence of possible spontaneous emission elimination. The physics behind atom pumping with a classical low-frequency field in the weak field approximation or a quantized low-frequency field consists in the fact that in the first case only modulation of the transition frequency occurs which does not affect the spontaneous emission in free space, while in the second case additional transitions are induced that may interfere leading to modification of the spontaneous decay. Particularly, in Ref. [17] a quantized low-frequency strong field was interacting with a two-level atom being initially in its excited state $|2\rangle$. To adequately describe the system the far-off resonant coupling to the other states was included as well.

In what follows, we recall in a somewhat different simplified way how the additional terms due to off-resonant coupling may appear in the interaction Hamiltonian. If as an example one considers a two-level atom with one extra far off-resonant state $|3\rangle$ and with its energy levels from down to up denoted as $|1\rangle$, $|2\rangle$, and $|3\rangle$, respectively, then the quantized low-frequency applied field will induce additional transitions via the path $|2\rangle \rightarrow |3\rangle \rightarrow |1\rangle$. To involve the corresponding terms one needs to go beyond the weak low-frequency field approximation applied in the main part of this work. The interaction Hamiltonian responsible for these terms is

$$H_I \approx -2i(c + c^\dagger) \sum_k (\vec{g}_k \cdot \vec{d}_{31}) \alpha_{32} (a_k^\dagger S^- - a_k S^+). \quad (\text{B1})$$

Here $\alpha_{ij} \propto d_{ij} E_L$ are the corresponding coefficients due to strong external pumping and obtained after elimination of the far-laying excited level $|3\rangle$, while $c^\dagger(c)$ is the photon creation (annihilation) operator for the external low-frequency quantized intense field. One can show (see the last entry of Ref. [17]) that the Hamiltonian (B1) does not affect the transition $|2\rangle \rightarrow |1\rangle$ when it is dipole allowed. Therefore, the spontaneous emission modification scheme described in this part applies to dipole-forbidden atomic transitions. Since in a three-level atomic system one transition should be dipole-forbidden it results that the decay on $|2\rangle \rightarrow |1\rangle$ atomic

transition may indeed be dipole-forbidden. The excited state population will be described by the following equation:

$$\frac{d}{dt}\langle S_{22} \rangle = -\gamma_b \langle S_{22} \rangle - \gamma_a \langle S_{22} (ce^{-i\omega t} + c^\dagger e^{i\omega t})^2 \rangle. \quad (\text{B2})$$

Here, γ_b is the two-photon spontaneous decay rate on transition $|2\rangle \rightarrow |1\rangle$, while γ_a is the corresponding decay involving additional upper states. One can observe that the strong quantized field indeed modifies the upper state population. Notice that a strong classical low-frequency laser field will only modulate the frequency on a dipole-allowed transition, and correspondingly, the spontaneous emission will not be modified in free space (see also Appendix A). For dipole-forbidden $|1\rangle \leftrightarrow |2\rangle$ transitions the off-resonant coupling to another state $|3\rangle$ will also modulate the transition frequency as well as induce transitions to the ground state $|1\rangle$ based on a Hamiltonian of the next form

$$H_I \approx -i \sum_k (\vec{g}_k \cdot \vec{d}_{31}) \alpha_{32} (a_k^\dagger S^- - a_k S^+) \cos(\omega t). \quad (\text{B3})$$

The spontaneous decay rate on the $|2\rangle \rightarrow |1\rangle$ atomic transition may be $\gamma_b + \alpha_{32}^2 \gamma_{31}$. Therefore, the classical off-resonant

coupling to another state may not change significantly the decay rate because $\alpha_{32} < 1$.

In a two-level atomic system with two extra far off-resonant states, the spontaneous emission can be modified due to an applied strong quantized low-frequency field even on a dipole-allowed $|2\rangle \leftrightarrow |1\rangle$ transition in accordance with the results given in Ref. [17]. For instance, one of the terms in the total Hamiltonian describing the decay via the path $|2\rangle \rightarrow |4\rangle \rightarrow |3\rangle \rightarrow |1\rangle$ after the elimination of the additional higher energy levels is

$$H_I \approx i(c + c^\dagger)^2 \sum_k (\vec{g}_k \cdot \vec{d}_{31}) \alpha_{24} \alpha_{43} (a_k^\dagger S^- - a_k S^+). \quad (\text{B4})$$

Such terms are responsible for the spontaneous decay modification in free space through a quantized and strong low frequency applied field. On the other side, in an idealized situation of ignoring the presence of any other far-off resonant states in the atomic system and when neglecting strong field terms of the low-frequency field, the presence of such interference terms could not be reproduced via a classical pumping field.

-
- [1] G. S. Agarwal, *Quantum Statistical Theories of Spontaneous Emission and their Relation to Other Approaches* (Springer, Berlin, 1974).
 - [2] L. Allen and J. H. Eberly, *Optical Resonance and Two-Level Atoms* (Dover, New York, 1975).
 - [3] Z. Ficek and S. Swain, *Quantum Interference and Coherence: Theory and Experiments* (Springer, Berlin, 2005).
 - [4] M. Kiffner, M. Macovei, J. Evers, and C. H. Keitel, *Progress in Optics* **55**, 85 (2010).
 - [5] B. W. Adams, C. Buth, S. Cavaletto, J. Evers, Z. Harman, C. H. Keitel, A. Palffy, A. Picon, R. Röhlsberger, Y. Rostovtsev, and K. Tamasaku, *J. Mod. Opt.* **60**, 2 (2013).
 - [6] S. Cavaletto, Z. Harman, C. Ott, C. Buth, T. Pfeifer, and C. H. Keitel, *Nat. Photon.* **8**, 520 (2014).
 - [7] D. F. Walls and G. J. Milburn, *Quantum Optics* (Springer-Verlag, Berlin, 1994).
 - [8] M. Nielsen and I. Chuang, *Quantum Computation and Quantum Information* (Cambridge University Press, Cambridge, England, 2000).
 - [9] E. M. Purcell, *Phys. Rev.* **69**, 681 (1946).
 - [10] D. Kleppner, *Phys. Rev. Lett.* **47**, 233 (1981).
 - [11] P. Goy, J. M. Raimond, M. Gross, and S. Haroche, *Phys. Rev. Lett.* **50**, 1903 (1983).
 - [12] E. Yablonovitch, *Phys. Rev. Lett.* **58**, 2059 (1987).
 - [13] S. John and T. Quang, *Phys. Rev. A* **50**, 1764 (1994); *Phys. Rev. Lett.* **74**, 3419 (1995).
 - [14] S. Noda, M. Fujita, and T. Asano, *Nat. Photon.* **1**, 449 (2007).
 - [15] E. Frishman and M. Shapiro, *Phys. Rev. Lett.* **87**, 253001 (2001); *Phys. Rev. A* **68**, 032717 (2003).
 - [16] L. Viola and S. Lloyd, *Phys. Rev. A* **58**, 2733 (1998).
 - [17] J. Evers and C. H. Keitel, *Phys. Rev. Lett.* **89**, 163601 (2002); *J. Phys. B: At. Mol. Opt. Phys.* **37**, 2771 (2004); U. Akram, J. Evers, and C. H. Keitel, *ibid.* **38**, L69 (2005).
 - [18] J. Evers and C. H. Keitel, *Phys. Rev. Lett.* **92**, 159303 (2004); A. G. Kofman, *ibid.* **92**, 159302 (2004); P. R. Berman, *ibid.* **92**, 159301 (2004).
 - [19] S.-Y. Zhu and M. O. Scully, *Phys. Rev. Lett.* **76**, 388 (1996); M. A. G. Martinez, P. R. Herczfeld, C. Samuels, L. M. Narducci, and C. H. Keitel, *Phys. Rev. A* **55**, 4483 (1997); H. Lee, P. Polynkin, M. O. Scully, and S.-Y. Zhu, *ibid.* **55**, 4454 (1997); E. Paspalakis and P. L. Knight, *Phys. Rev. Lett.* **81**, 293 (1998); C. H. Keitel, *ibid.* **83**, 1307 (1999).
 - [20] K. P. Heeg, H.-C. Wille, K. Schlage, T. Guryeva, D. Schumacher, I. Uschmann, K. S. Schulze, B. Marx, T. Kämpfer, G. G. Paulus, R. Röhlsberger, and J. Evers, *Phys. Rev. Lett.* **111**, 073601 (2013).
 - [21] U. D. Jentschura, J. Evers, M. Haas, and C. H. Keitel, *Phys. Rev. Lett.* **91**, 253601 (2003).
 - [22] Z.-H. Li, D.-W. Wang, H. Zheng, S.-Y. Zhu, and M. S. Zubairy, *Phys. Rev. A* **82**, 050501(R) (2010).
 - [23] G. S. Agarwal, *Phys. Rev. A* **61**, 013809 (1999).
 - [24] M. Janowicz, *Phys. Rev. A* **61**, 025802 (2000).
 - [25] A. G. Kofman and G. Kurizki, *Phys. Rev. Lett.* **87**, 270405 (2001).
 - [26] G. S. Agarwal, M. O. Scully, and H. Walther, *Phys. Rev. Lett.* **86**, 4271 (2001).
 - [27] Y. V. Radeonychev, M. D. Tokman, A. G. Litvak, and O. Kocharovskaya, *Phys. Rev. Lett.* **96**, 093602 (2006); Y. V. Radeonychev, V. A. Polovinkin, and O. Kocharovskaya, *ibid.* **105**, 183902 (2010); V. A. Antonov, Y. V. Radeonychev, and O. Kocharovskaya, *ibid.* **110**, 213903 (2013).
 - [28] M. W. Noel, W. M. Griffith, and T. F. Gallagher, *Phys. Rev. A* **58**, 2265 (1998).
 - [29] V. A. Kovarskii and O. B. Prepelitsa, *Opt. Spectrosc.* **90**, 351 (2001).
 - [30] O. V. Kibis, G. Y. Slepyan, S. A. Maksimenko, and A. Hoffmann, *Phys. Rev. Lett.* **102**, 023601 (2009).

- [31] F. Oster, C. H. Keitel, and M. Macovei, *Phys. Rev. A* **85**, 063814 (2012).
- [32] I. G. Savenko, O. V. Kibis, and I. A. Shelykh, *Phys. Rev. A* **85**, 053818 (2012).
- [33] E. Paspalakis, J. Boviatsis, and S. Baskoutas, *J. Appl. Phys.* **114**, 153107 (2013).
- [34] W. Yang, X. Song, C. Zhang, and Z. Xu, *J. Phys. B: At. Mol. Opt. Phys.* **42**, 175601 (2009).
- [35] M. Metcalfe, S. M. Carr, A. Muller, G. S. Solomon, and J. Lawall, *Phys. Rev. Lett.* **105**, 037401 (2010).
- [36] S. N. Shevchenko, S. Ashhab, and F. Nori, *Phys. Rep.* **492**, 1 (2010); S. N. Shevchenko, A. N. Omelyanchouk, and E. Il'ichev, *Low. Temp. Phys.* **38**, 283 (2012).
- [37] G. Lindblad, *Commun. Math. Phys.* **48**, 119 (1976).
- [38] S. M. Barnett and S. Stenholm, *Phys. Rev. A* **64**, 033808 (2001).
- [39] E. Janke, F. Emde, and F. Lösch, *Tafeln Höherer Functionen* (B. G. Teubner Verlagsgesellschaft, Stuttgart, Germany, 1960).